SCIENTIFIC OASIS

Spectrum of Mechanical Engineering and Operational Research

Journal homepage: www.smeor-journal.org
eISSN: 3042-0288

A Spatial-Simulation-MCDM Framework for Prioritizing Vaccine Cold-Chain Resilience Strategies in Libya

Ibrahim Badi[1*], Osama Serrar[2]

[1] Department of Mechanical Engineering, Libyan Academy-Misrata, Libya
[2] Faculty of Pharmacy, Misurata University, Libya

ARTICLE INFO

Article history:
Received 31 May 2026
Received in revised form 7 July 2026
Accepted 9 September 2026
Available online 13 September 2026

Keywords:
Vaccine Cold Chain; Spatial Accessibility; Monte Carlo Simulation; BWM; TOPSIS; Resilience; Health Logistics

ABSTRACT

Vaccine cold chains preserve vaccine potency across storage, transport, and service-delivery points. In geographically dispersed health systems, cold-chain planning requires spatial, operational, and strategic evidence because storage failure, transport delay, and demand pressure can affect service continuity. This study proposes a decision-support framework for prioritizing vaccine cold-chain resilience strategies in Libya. The framework integrates city-level spatial screening of twenty principal urban centers, Monte Carlo disruption simulation, and a BWM-TOPSIS model informed by a four-expert assessment. The analysis separates calculated spatial indicators, structured screening scores, and expert elicitation inputs, and reports the simulation parameters, BWM comparison vectors, TOPSIS scoring procedure, consistency results, comparative ranking checks, and rank-reversal tests. Results place southern and southeastern cities at the upper end of the cold-chain vulnerability ranking and identify preventive maintenance and spare parts, digital temperature monitoring, and route planning with emergency redistribution protocols as the leading resilience package. The framework offers a transparent and updateable basis for cold-chain planning in Libya and comparable settings.

1. Introduction

Vaccination is one of the most cost-effective public health interventions, but its effectiveness depends not only on vaccine procurement and clinical delivery but also on the integrity of the cold chain that connects national stores, intermediate storage points, transport operations, and service-delivery facilities [1]. Most routine vaccines must be protected within controlled temperature ranges during storage and distribution, and failures in refrigeration, monitoring, handling, or transport can reduce potency, increase wastage, and weaken public confidence in immunization programmes. For countries with large territories, uneven population distribution, fragile infrastructure, and limited administrative data, the cold chain should be understood as a resilience problem rather than a purely technical storage problem [2].

Libya provides a relevant context for such an analysis. The country combines a large geographic area with a population concentrated along the northern coast and smaller, dispersed settlements

* *Corresponding author.*
E-mail address: i.badi@lam.edu.ly

https://doi.org/10.31181/smeor41202760

across the interior and south [3]. This spatial configuration affects transport times, access to maintenance services, the availability of reliable electricity, and the ability of national or regional health authorities to monitor vaccine storage conditions across different levels of the system. Recent WHO reporting on Libya's National Immunization Programme Review identifies cold-chain logistics, service delivery, disease surveillance, community outreach, and data quality as components of programme assessment [4]. This indicates that cold-chain logistics remains part of the current policy discussion on immunization performance in Libya.

The Libyan Expanded Programme on Immunization has a long institutional history and has expanded from early vaccination activities in the 1960s to a programme that currently immunizes against seventeen infectious diseases [5]. Nevertheless, the existence of a national programme does not eliminate operational heterogeneity [6]. Coverage, access, and service continuity may differ substantially between coastal metropolitan areas and remote municipalities. This means that the policy problem is not simply whether vaccines are nationally available, but whether the cold chain can remain reliable under everyday disruptions and emergency conditions across diverse spatial settings.

The literature on vaccine cold chains emphasizes several recurring challenges in low- and middle-income countries [7, 8]. These include inadequate or aging cold-chain equipment, unreliable electricity supply, weak temperature monitoring, limited preventive maintenance, delayed distribution, insufficient storage capacity during campaigns, and shortage of trained personnel. Technological innovations such as solar direct-drive refrigerators, freeze-free carriers, remote temperature monitoring, voltage stabilization, and improved passive cooling devices have expanded the set of feasible interventions [9, 10]. However, these technologies must be prioritized according to local risk, affordability, implementation speed, operational feasibility, and equity rather than selected solely on technical performance.

A second stream of literature concerns spatial accessibility in health service delivery. Geographic accessibility analysis is commonly used to identify underserved populations, evaluate travel-time burdens, and support the targeting of health resources [11]. In immunization planning, geospatial approaches can help identify missed settlements, zero-dose populations, and areas where routine services may be logistically fragile [11]. High-resolution GIS modelling usually requires detailed road networks, catchment boundaries, facility locations, population grids, and service data. These inputs are not consistently available in the Libyan cold-chain context. For early planning, simpler spatial indicators such as distance to reference distribution hubs, city location, remoteness, and regional transport difficulty can provide a transparent first screening layer.

A third relevant stream is simulation modelling for health logistics and supply-chain resilience. Simulation enables planners to examine how systems behave under uncertainty, including demand surges, power failures, transport delays, equipment breakdowns, and emergency campaigns [12, 13]. Detailed discrete-event or agent-based models can be valuable when high-frequency operational records exist. In this study, Monte Carlo simulation is used for a narrower purpose: to translate bounded ranges for power, transport, and demand disruption into comparable city-level exposure scores. This use is appropriate for a first screening stage because the distribution parameters can be stated explicitly.

Multi-criteria decision-making (MCDM) has also been widely applied in health strategies [14, 15], supplier selection [16], technology choice, and infrastructure prioritization [17]. In vaccine cold-chain studies, MCDM has been used to evaluate logistics service providers, select digital or technological solutions, and rank performance improvement options. The Best-Worst Method (BWM) is attractive because it reduces the number of pairwise comparisons required from decision-makers and includes a consistency logic [18, 19]. TOPSIS is also appropriate for this problem because it ranks alternatives according to their relative closeness to a positive ideal and distance from a negative ideal, which fits problems involving trade-offs among benefits, costs, feasibility, and sustainability [20].

By coupling spatial screening and disruption simulation with the MCDM stage, the framework links the strategy ranking to the geographic and operational conditions under which vaccine distribution takes place. The ranking is therefore interpreted in relation to accessibility, power exposure, transport constraints, and demand pressure, rather than as a stand-alone preference exercise.

A methodological gap remains between high-resolution optimization models that require extensive operational data and expert-based MCDM studies that rank strategies without considering spatial or disruption exposure. In fragile or data-constrained systems, decision-makers may first need a planning-level framework that documents the origin of each input and can be implemented with city-level information. Such a framework can support early investment discussions, reveal which data gaps matter most, and prepare the ground for more detailed assessments later.

This paper addresses that gap by proposing a spatial-simulation-MCDM framework for prioritizing vaccine cold-chain resilience strategies in Libya. The framework first constructs a spatial vulnerability profile for twenty principal urban centers using nearest-hub distance, demand proxy, power-risk score, and transport-risk score. It then applies Monte Carlo simulation to estimate disruption exposure under power, transport, and demand uncertainty. Finally, it uses BWM-derived criteria weights and TOPSIS to rank strategies that strengthen the current cold-chain system through equipment, monitoring, maintenance, transport, and staff-practice improvements.

The paper contributes by showing how city-level spatial indicators, disruption ranges, and expert-informed MCDM judgments can be connected in one reproducible workflow. The methodological contribution is the explicit integration of geographic accessibility, operational disruption exposure, and strategy prioritization. The practical contribution lies in identifying a focused set of cold-chain resilience actions that warrant early policy and operational attention in Libya, including preventive maintenance, digital temperature monitoring, route-planning improvements, staff training, passive transport kits, and targeted backup-energy support. These strategies are intended to strengthen the reliability, continuity, and equity of vaccine delivery and to guide more detailed investment appraisal when facility-level records become available.

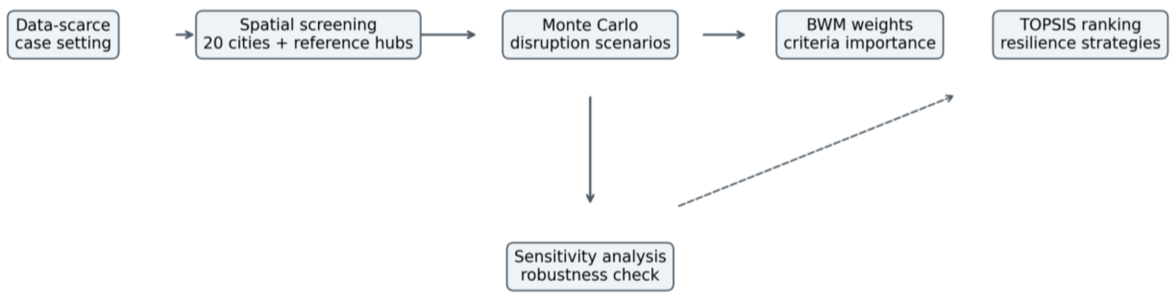

Fig. 1. Proposed spatial-simulation-MCDM framework

Figure 1 presents the operational sequence of the framework. The first block defines the available-data case setting; the second block converts city locations and operational screening scores into a spatial dataset; the third block uses Monte Carlo simulation to translate uncertainty in power, transport, and demand into disruption exposure; and the fourth block applies BWM-derived weights and TOPSIS to rank the seven resilience strategies. The sensitivity-analysis block is linked to both the simulation and MCDM stages because it tests the stability of the main conclusions under alternative criterion-weighting conditions.

2. Methodology

2.1 Research design

The study proposes an integrated decision-support framework for vaccine cold-chain resilience in Libya. The framework organizes spatial information, operational-risk screening scores, stochastic disruption analysis, and expert-based strategy evaluation into one replicable sequence. The design supports early resilience planning in contexts where facility inventories, transport logs, temperature histories, and municipal demand records are collected unevenly across institutions.

The framework has four operational stages. Stage 1 defines the city set and reference distribution hubs. Stage 2 converts each city into comparable spatial and operational-risk indicators. Stage 3 uses these indicators to parameterize the Monte Carlo distributions and compute disruption exposure. Stage 4 uses the resulting risk profile to structure the BWM-TOPSIS evaluation of resilience strategies. The transition between stages is operationally linked: distance and risk-screening scores inform the simulation, and the vulnerability profile informs the interpretation of the strategy ranking.

The framework distinguishes between three categories of inputs: calculated spatial indicators, literature- and public-source-supported contextual inputs, and structured expert assessments. City coordinates and hub distances are treated as calculated inputs. The demand proxy, power-risk score, and transport-risk score are treated as ordinal screening inputs derived from predefined coding rules. The BWM comparison vectors and TOPSIS performance scores are based on a four-expert elicitation process involving expertise in logistics, vaccine handling, and cold-chain operations, using the criteria and strategy definitions reported in the paper.

The city-level input values were developed through a structured coding procedure and reviewed by the four experts. The experts first examined the city-level screening dataset and then completed the BWM and TOPSIS assessment forms. Differences in coding or scoring were discussed with reference to the variable definitions and scoring anchors until an agreed value was reached. The distance to the nearest reference hub was calculated directly from city coordinates, while the accessibility-risk score was produced by the linear transformation reported in Section 2.2. Table 1 shows the basis for city-level input values and coding procedure.

Table 1
Basis for city-level input values and coding procedure

Input variable	Derivation or coding rule	Scale/status	Role in the framework
City coordinates	Public geographic coordinates of the selected principal urban centers.	Calculated/public spatial data	Used to compute nearest-hub distance and prepare the spatial map.
Reference hubs	Tripoli, Benghazi, Misrata, and Sabha were selected as analytical reference nodes representing major national and regional logistical poles.	Expert-supported analytical choice	Used to estimate relative accessibility from each city to distribution capacity.
Distance to nearest hub	Minimum haversine distance from each city to the four reference hubs.	Calculated value in km	Primary continuous indicator of spatial remoteness.
Accessibility-risk score	Continuous rescaling of nearest-hub distance to a 1-5 score using Equation (3); no quantile breaks were used.	Calculated screening score	Allows distance to be combined with other ordinal risk indicators.
Demand proxy	Five-point ordinal coding based on relative city size and role as a service center; higher values indicate larger expected immunization workload.	Structured screening score	Represents pressure on storage, stock control, and delivery continuity.

Table 1
Continued

Input variable	Derivation or coding rule	Scale/status	Role in the framework
Power-risk score	Five-point ordinal coding reflecting expected electricity vulnerability, remoteness, and continuity concerns.	Structured screening score	Drives the power-exposure component in the Monte Carlo model.
Transport-risk score	Five-point ordinal coding reflecting route difficulty, distance from logistics support, and emergency redistribution constraints.	Structured screening score	Drives the transport-exposure component in the Monte Carlo model.
Strategy performance scores	Aggregated four-expert assessment of each strategy against each criterion using the 1-9 anchors reported in Table 5.	Four-expert assessment	Provides the decision matrix used in TOPSIS.

The coding protocol separates calculated values from expert-elicited screening scores so that the role of each input is visible in the workflow. This structure also allows the model to be rerun when facility records, electronic temperature logs, transport data, or updated expert assessments become available.

2.2 Spatial screening

The spatial component is conducted at the city level in order to provide a practical and scalable basis for assessing cold-chain accessibility across Libya. This level of analysis captures broad spatial disparities while keeping the data requirements lower than a complete geodatabase of health facilities, cold rooms, refrigerators, road segments, and vaccine flows. Four reference distribution hubs are considered in the screening process: Tripoli, Benghazi, Misrata, and Sabha. These hubs represent major urban and logistical poles within the national health-supply network and serve as analytical reference nodes for estimating relative accessibility. For each city, the distance to the nearest reference hub is calculated using the haversine great-circle distance formula. The resulting distance is converted into an accessibility-risk score ranging from 1 to 5, where higher values indicate greater remoteness and weaker spatial access to distribution capacity.

In addition to spatial distance, the model incorporates two operational risk indicators: power-risk score and transport-risk score. Both indicators are measured on a five-point scale and reflect the relative exposure of each city to electricity instability and transport difficulty. These indicators extend the analysis beyond geographic remoteness by capturing operational conditions that directly affect the reliability of vaccine storage and distribution. The combined use of accessibility, power-risk, and transport-risk scores provides a structured basis for identifying cities with higher cold-chain vulnerability and for linking spatial conditions with resilience-oriented decision-making.

The accessibility-risk score is calculated from the distance variable. For each city, the great-circle distance to each reference hub is obtained using the haversine equation. The nearest-hub distance is then transformed into a continuous accessibility-risk score through linear rescaling. The rescaling assigns a value of 1 to a city located at a reference hub and a value of 5 to the most remote city in the selected city set; therefore, no quantile breaks or categorical distance thresholds are used.

$$d_{ih} = 2R\sin^{-1}\left(\sqrt{\sin^2\left(\frac{\phi_h-\phi_i}{2}\right) + \cos(\phi_i)\cos(\phi_h)\sin^2\left(\frac{\lambda_h-\lambda_i}{2}\right)}\right) \tag{1}$$

$$d_i = \min_h(d_{ih}) \tag{2}$$

$$AR_i = 1 + 4\left(\frac{d_i}{d_{\max}}\right) \tag{3}$$

where d_{ih}denotes the great-circle distance between city $i$and reference hub h; $R$is the mean radius of the Earth, taken as 6,371 km; $\phi_i$and $\phi_h$denote the latitudes of city $i$and hub h, respectively; $\lambda_i$and $\lambda_h$denote the longitudes of city $i$and hub h, respectively; and all latitude and longitude values are expressed in radians. The term $d_i$represents the distance from city $i$to its nearest reference hub, while $d_{\max}$denotes the largest nearest-hub distance among all selected cities. Finally, $AR_i$is the accessibility-risk score of city i, rescaled from 1 to 5, where a higher value indicates weaker spatial accessibility to the reference distribution hubs.

2.3 Monte Carlo disruption simulation

The simulation component estimates a disruption exposure index for each city. Three uncertain variables are considered: power outage exposure, transport delay, and demand surge. Power outage exposure is modelled as a triangular distribution whose parameters increase with the power-risk score. Transport delay is modelled as a triangular distribution whose parameters increase with the transport-risk and accessibility-risk scores. Demand surge is modelled as a triangular multiplier influenced by the demand proxy. The triangular distribution is selected because it is transparent and suitable when only minimum, most likely, and maximum values can be elicited from experts.

For each city, 5,000 Monte Carlo iterations are performed to simulate variation in operational disruption conditions. In each iteration, the normalized values of power exposure, transport delay, and demand surge are aggregated into a disruption exposure score. This score provides an operational risk indicator that reflects the combined effect of electricity instability, transport uncertainty, and demand fluctuation on vaccine cold-chain continuity. The probability of high disruption is then calculated as the proportion of simulated iterations that exceed the predefined disruption threshold. Accordingly, the simulation produces two main outputs for each city: the average disruption exposure score and the probability of experiencing a high-disruption condition. These outputs provide a quantitative basis for comparing cities and linking operational uncertainty with the subsequent prioritization of resilience strategies.

To support reproducibility, the Monte Carlo model uses 5,000 iterations for each city. The power component is drawn from the triangular distribution assigned to the city power-risk score. The transport component is drawn from a triangular distribution based on a combined transport-accessibility index. The demand component is drawn from the triangular distribution assigned to the city demand proxy. The disruption exposure score is obtained as a weighted aggregation of the three components, and the probability of high disruption is calculated as the percentage of iterations in which disruption exposure reaches the specified threshold.

$$t_i^* = 0.60TR_i + 0.40AR_i \tag{4}$$

$$T_i \sim Tri(8 + 10t_i^*, 13 + 12t_i^*, 18 + 14t_i^*) \tag{5}$$

$$E_{i,k} = 0.40P_{i,k} + 0.40T_{i,k} + 0.20D_{i,k} \tag{6}$$

$$H_i = 100 \times \frac{n(E_{i,k} \geq 55)}{5000} \tag{7}$$

where $i$denotes the city index and $k$denotes the Monte Carlo iteration, with $k = 1,2,\ldots,5000$. $TR_i$is the transport-risk score of city i, and $AR_i$is the accessibility-risk score of city i. The term t_i^*represents the combined transport-accessibility index used to parameterize the transport-delay distribution. $T_{i,k}$is the simulated transport-delay exposure of city $i$in iteration k, generated from a triangular distribution $Tri(a, b, c)$, where a, b, and $c$represent the minimum, most likely, and maximum values, respectively. $P_{i,k}$, $T_{i,k}$, and $D_{i,k}$denote the simulated power-outage exposure, transport-delay exposure, and demand-pressure exposure of city $i$in iteration k, respectively. $E_{i,k}$is the disruption exposure score of city i in iteration k, calculated as a weighted aggregation of the three simulated components. H_i is the probability of high disruption for city i, expressed as a percentage. The notation $n(E_{i,k} \geq 55)$ denotes the number of Monte Carlo iterations in which the disruption exposure score of city i is equal to or greater than the threshold value of 55. The value 5000 is the total number of simulation iterations used for each city.

The composite vulnerability score is computed after standardizing the ordinal accessibility, power-risk, and transport-risk scores to a common 0-100 scale. The final screening index combines standardized accessibility risk, mean disruption exposure, high-disruption probability, standardized power risk, and standardized transport risk. This aggregation gives the highest emphasis to simulated disruption exposure and accessibility while retaining the two expert-screened operational-risk indicators.

$$X_i^* = 25(X_i - 1) \tag{8}$$

$$V_i = 0.25AR_i^* + 0.30\bar{E}_i + 0.20H_i + 0.125PR_i^* + 0.125TR_i^* \tag{9}$$

where X_i is an original 1–5 risk score for city i, and X_i^* is its standardized value on a 0–100 scale. In Equation (9), AR_i^*, PR_i^*, and TR_i^* denote the standardized accessibility-risk, power-risk, and transport-risk scores, respectively. E_i represents the mean simulated disruption exposure score, H_i represents the probability of high disruption, and V_i is the composite vulnerability score for city i. The aggregation coefficients in Equation (9) sum to one and define the relative contribution of each component to the final city-level vulnerability score.

2.4 BWM-TOPSIS decision model

The decision model prioritizes seven resilience strategies selected for near- to medium-term implementability within the existing cold-chain system: solar direct-drive refrigerators for high-risk facilities, backup power and voltage stabilization, digital temperature monitoring, preventive maintenance and spare parts, route planning and emergency redistribution, training and standard operating procedures, and passive cold boxes with emergency transport kits. The strategy set emphasizes actions that can improve reliability through equipment functionality, monitoring, staff practice, transport coordination, and targeted energy support, while larger construction projects are left for subsequent facility-level investment planning.

Eight criteria are used: risk reduction, spatial equity, cost efficiency, implementation speed, operational feasibility, monitoring and data improvement, sustainability, and emergency response value. BWM is used to obtain criteria weights because it requires fewer comparisons than full pairwise comparison methods and is suitable for expert elicitation [18]. TOPSIS is then used to rank the strategies. Since all criteria are expressed as benefit scores from 1 to 9, the positive ideal solution contains the best score for each criterion and the negative ideal solution contains the worst score. The closeness coefficient is calculated for each strategy, and the alternatives are ranked from highest to lowest coefficient.

$$\min \xi \tag{10}$$

$$\left|w_B - a_{Bj}w_j\right| \leq \xi, \quad \left|w_j - a_{jW}w_W\right| \leq \xi, \quad \textstyle\sum_j w_j = 1, \quad w_j \geq 0 \tag{11}$$

where w_j denotes the weight of criterion j, w_B denotes the weight of the best criterion, and w_W denotes the weight of the worst criterion. a_{Bj} represents the preference of the best criterion B over criterion j, while a_{jW} represents the preference of criterion j over the worst criterion W. The parameter ξ is the maximum absolute deviation minimized in the BWM model and is used to evaluate the consistency of the aggregated comparison vector. The constraint $\sum_j w_j = 1$ensures that all criteria weights sum to one, while $w_j \geq 0$ ensures non-negative weights for all criteria.

The scoring anchors and rationale are reported in Tables 5 and 6, while the final performance matrix is presented in Table 12. A higher value means that the strategy contributes more strongly to the criterion. For cost efficiency, a higher score denotes a better expected benefit relative to investment and recurrent cost, not a higher cost. The verbal anchors and strategy-level scoring rationale are provided in Tables 5 and 6.

For TOPSIS, the decision matrix is vector-normalized and then multiplied by the BWM criteria weights. Because all criteria are benefit criteria, the positive and negative ideal values are denoted as Pj and Nj, respectively. Each strategy is then ranked according to its relative closeness to the positive ideal solution.

$$r_{ij} = \frac{x_{ij}}{\sqrt{\sum_i x_{ij}^2}} \tag{12}$$

$$v_{ij} = w_j r_{ij} \tag{13}$$

$$P_j = \max_i(v_{ij}), \quad N_j = \min_i(v_{ij}) \tag{14}$$

$$D_i^P = \sqrt{\sum_j (v_{ij} - P_j)^2}, \quad D_i^N = \sqrt{\sum_j (v_{ij} - N_j)^2} \tag{15}$$

$$CC_i = \frac{D_i^N}{D_i^P + D_i^N} \tag{16}$$

where x_{ij}denotes the original performance score of strategy $i$with respect to criterion j, and r_{ij}denotes the normalized value obtained by vector normalization. v_{ij}represents the weighted normalized performance value, calculated by multiplying $r_{ij}$by the BWM-derived criterion weight w_j. $P_j$and $N_j$denote the positive ideal and negative ideal values for criterion j, respectively. Since all criteria are treated as benefit criteria, $P_j$is the maximum weighted normalized value for criterion j, while $N_j$is the minimum weighted normalized value. S_i^+represents the Euclidean distance of strategy $i$from the positive ideal solution, and S_i^-represents its Euclidean distance from the negative ideal solution. Finally, CC_idenotes the TOPSIS closeness coefficient of strategy i, where a higher CC_iindicates that the strategy is closer to the positive ideal solution and farther from the negative ideal solution. Strategies are ranked in descending order of CC_i.

2.5 Expert elicitation and calculation details

Tables 2, 3, 4, 5, 6 and 7 report the calculation details used to reproduce the analysis: proxy-risk score meanings, Monte Carlo parameters, aggregated BWM vectors, TOPSIS scoring anchors, strategy-level scoring rationale, and intermediate TOPSIS values. Together with Table 1, these tables document how calculated spatial data, expert-screened inputs, and MCDM judgments enter the model.

The accessibility-risk score was calculated using Equation (3). The conversion is a continuous linear rescaling and does not use quantile breaks. This choice preserves proportional distance differences among cities while keeping all risk indicators on a comparable 1-5 scale. Table 2 explains the proxy operational-risk scores.

For BWM, the four-expert assessment selected C1 risk reduction as the best criterion and C8 emergency response value as the least influential criterion in the weighting step. The aggregated best-to-others vector and the aggregated others-to-worst vector are reported in Table 4. The BWM weights are obtained by minimizing the maximum absolute deviation subject to the standard BWM constraints. The resulting consistency deviation is 0.006, which indicates highly consistent comparisons for the aggregated vector.

Table 2
Interpretation of proxy operational-risk scores

Score	Power-risk interpretation	Transport-risk interpretation
1	Low exposure; stable electricity and limited voltage disruption expected	Low transport difficulty; short and reliable access to hub routes
2	Moderate-low exposure; occasional disruption but manageable at city level	Moderate-low route difficulty and generally reliable redistribution
3	Moderate exposure; interruptions may affect cold-chain continuity without backup procedures	Moderate route difficulty, longer travel time, or weaker redistribution options
4	High exposure; frequent instability requiring backup and maintenance planning	High transport difficulty due to distance, route constraints, or limited redundancy
5	Very high exposure; power instability is a central cold-chain risk	Very high transport difficulty and weak emergency redistribution flexibility

The distribution values used for the simulation are reported in Table 3.

Table 3
Monte Carlo model specification

Variable	Risk driver	Triangular parameter rule	Scale
Power exposure component	Power-risk score on the 1-5 screening scale	Score 1: (5, 10, 20); Score 2: (20, 30, 45); Score 3: (35, 45, 60); Score 4: (50, 60, 75); Score 5: (65, 75, 90)	0-100
Transport exposure component	Combined transport-accessibility index defined in Equation (4)	Distribution generated according to Equation (5)	0-100
Demand-pressure component	Demand proxy on the 1-5 screening scale	Score 1: (0, 5, 10); Score 2: (5, 10, 20); Score 3: (10, 20, 30); Score 4: (15, 30, 45); Score 5: (20, 40, 60)	0-100
Disruption exposure score	Power, transport, and demand components	Weighted aggregation calculated according to Equation (6)	0-100
High-disruption event	Disruption exposure threshold	Percentage of iterations calculated according to Equation (7)	%

Table 4
Aggregated BWM comparison vectors and final weights

Criterion	C1	C2	C3	C4	C5	C6	C7	C8
Best-to-Others vector (best = C1)	1.00	1.44	1.77	1.92	1.53	2.88	2.88	4.60
Others-to-Worst vector (worst = C8)	4.60	3.20	2.60	2.40	3.00	1.60	1.60	1.00
Final normalized weight	0.230	0.160	0.130	0.120	0.150	0.080	0.080	0.050

C1 was selected as the best criterion because reducing vaccine loss and service disruption is the central resilience objective. C8 was selected as the least influential criterion in the weighting step because emergency-response value partly overlaps with risk reduction and implementation speed. The final weights show that risk reduction, spatial equity, operational feasibility, cost efficiency, and implementation speed carry the main influence in the model. Table 5 shows the TOPSIS benefit-score interpretation.

Table 5
TOPSIS benefit-score interpretation

Score	Interpretation used for TOPSIS scoring
1	Very weak contribution to the criterion
3	Weak contribution
5	Moderate contribution
7	Strong contribution
9	Very strong contribution

Intermediate values 2, 4, 6, and 8 were allowed when a strategy fell between two adjacent verbal levels. All eight criteria were treated as benefit criteria. For the cost-efficiency criterion, the score represents value for money: a score of 9 indicates a very favourable expected benefit relative to investment and recurrent cost. Table 6 presents the basis for TOPSIS performance scoring.

Table 6
Basis for TOPSIS performance scoring

Alternative	Main scoring rationale
A1	Strong technical risk reduction and sustainability for high-risk facilities, but lower speed and cost-efficiency because procurement, installation, and maintenance requirements are substantial
A2	High emergency value and feasibility where municipal stores exist, but weaker sustainability and data-improvement contribution than monitoring or maintenance options
A3	High monitoring/data improvement and fast implementation; moderate equity because benefits depend on network coverage and response capacity
A4	Strong risk reduction, cost efficiency, feasibility, and sustainability because it improves reliability of existing cold-chain assets
A5	High equity and emergency-response value because redistribution and route planning help remote municipalities and temporary disruptions
A6	High cost efficiency and implementation speed; lower direct technical risk reduction than equipment, monitoring, or maintenance investments
A7	High equity and emergency value during transport and campaigns; lower data-recording contribution because it does not create continuous monitoring records

Table 7 reports the TOPSIS distance and closeness values used to derive the final ranking.

Table 7
TOPSIS distance and closeness values

Strategy	Distance from positive ideal	Distance from negative ideal	Closeness coefficient
A1	0.0601	0.0402	0.4006
A2	0.0541	0.0283	0.3437
A3	0.0339	0.0496	0.5939
A4	0.0308	0.0471	0.6044
A5	0.0328	0.0472	0.5901
A6	0.0444	0.0514	0.5368
A7	0.0486	0.0409	0.4566

Note for Table 7. The distance and closeness columns are calculated from the weighted vector-normalized TOPSIS matrix using the equations reported in Section 2.4. The closeness coefficient is the value used to rank the strategies in Table 13.

The case application is designed for city-level resilience planning. It uses city locations, structured risk screening, simulation, and expert assessment to identify where attention is needed and which actions should be considered first. Facility-level audits, temperature records, cold-room inventories, vehicle data, and vaccine-flow records remain essential for procurement plans, detailed budgeting, and local implementation. In this role, the framework complements national Effective Vaccine Management assessments and facility-level cold-chain inventories. Table 8 presents the overview of the proposed framework, while Table 9 indicates the decision criteria and BWM-derived weights and Table 10 indicates the strategies evaluated.

Table 8
Overview of the proposed framework

Component	Main output
Spatial screening	City-level accessibility and vulnerability profile
Simulation	Disruption exposure and high-disruption probability
MCDM weighting	Relative importance of decision criteria
MCDM ranking	Priority ranking of resilience strategies
Sensitivity analysis	Stability of leading strategies under alternative weights

Table 9
Decision criteria and BWM-derived weights

Code	Criterion	Definition	Weight
C1	Risk reduction	Ability to reduce thermal exposure, stock loss, or service disruption	0.230
C2	Spatial equity	Ability to benefit remote and high-vulnerability municipalities	0.160
C3	Cost efficiency	Expected benefit relative to investment and recurrent cost	0.130
C4	Implementation speed	Potential to be implemented within a short planning horizon	0.120
C5	Operational feasibility	Compatibility with existing institutions, staff capacity, and procurement conditions	0.150
C6	Monitoring/data improvement	Contribution to real-time visibility, temperature records, and accountability	0.080
C7	Sustainability	Expected durability and maintainability after initial deployment	0.080
C8	Emergency response value	Usefulness during campaigns, outbreaks, power failures, or transport disruption	0.050

Table 10
Resilience strategies evaluated in the MCDM model

Code	Strategy
A1	Solar direct-drive vaccine refrigerators for high-risk facilities
A2	Backup power units and voltage stabilization for municipal cold stores
A3	Digital temperature monitoring and SMS/online alert system
A4	Preventive maintenance and spare-parts programme
A5	Route planning and emergency redistribution protocol
A6	Training and standard operating procedures for vaccine handlers
A7	Passive cold boxes, conditioned ice packs, and emergency transport kits

3. Results

The case application covers twenty principal urban centers distributed across Libya. The selection includes large coastal cities, eastern cities, central locations, mountain and interior cities, and remote southern and southeastern cities. The selected set was chosen to provide national spatial coverage rather than to enumerate all municipalities. This coverage allows the framework to distinguish between relatively accessible urban centers and remote locations where cold-chain resilience may require special attention.

The spatial map in Figure 2 shows that the selected cities cover the northern coastal corridor and the major interior and southern urban centers. The northern cities are generally closer to one of the reference hubs, whereas southern and southeastern cities require longer access distances and face higher combined operational-risk scores. This spatial dispersion is central to the logic of the model: a strategy with high cost-efficiency or rapid implementation in Tripoli or Benghazi may provide a different equity contribution in Kufra, Ghat, Ubari, Murzuq, or Sabha when last-mile redistribution and maintenance access are considered.

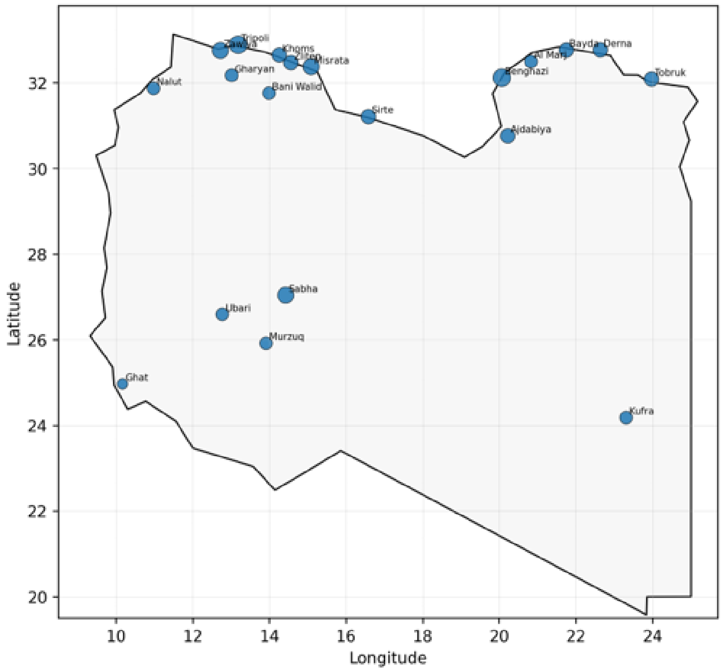

Fig. 2. Location of the twenty selected principal urban centers in Libya

The average disruption exposure reported in Table 11 is the mean disruption score across 5,000 iterations. The probability of high disruption is the percentage of iterations in which the disruption exposure score reaches the threshold defined in Equation (7).

Table 11
City-level spatial and simulated cold-chain vulnerability indicators

Rank	City	Region	NRH	DNH (km)	DP	ARS	PRS	TRS	SDE	PHD (%)	CVS
1	Kufra	Southeast	Benghazi	938.1	2	5.00	5	5	71.55	92.60	89.98
2	Ghat	Southwest	Sabha	483.7	1	3.06	5	5	68.02	87.22	75.72
3	Ubari	Southwest	Sabha	171.4	2	1.73	5	5	68.81	87.76	67.76
4	Murzuq	Southwest	Sabha	134.7	2	1.57	5	5	68.83	88.26	66.86
5	Sabha	Southwest	Sabha	0.0	4	1.00	5	5	71.88	91.82	64.93
6	Nalut	Western mountain	Tripoli	236.4	2	2.01	4	4	60.06	65.46	56.17
7	Bani Walid	Interior	Misrata	124.3	2	1.53	4	4	59.55	65.46	53.02
8	Tobruk	East	Benghazi	368.3	3	2.57	3	4	55.00	50.28	51.99
9	Derna	East	Benghazi	251.8	3	2.07	3	3	49.17	30.04	39.95
10	Sirte	Central	Misrata	191.9	3	1.82	3	3	48.91	28.06	37.91
11	Bayda	East	Benghazi	174.0	3	1.74	3	3	49.03	29.32	37.70
12	Ajdabiya	East	Benghazi	152.1	3	1.65	3	3	48.50	26.84	36.48
13	Khoms	Central coast	Misrata	83.4	3	1.36	2	2	34.17	0.34	18.82
14	Zawiya	Northwest	Tripoli	45.8	4	1.20	2	2	35.78	0.68	18.37
15	Gharyan	Mountain	Tripoli	81.1	2	1.35	2	2	32.29	0.08	18.14
16	Al Marj	East	Benghazi	83.0	2	1.35	2	2	32.17	0.06	18.10
17	Benghazi	East	Benghazi	0.0	5	1.00	2	2	37.54	1.74	17.86
18	Zliten	Central coast	Misrata	50.2	3	1.21	2	2	33.98	0.12	17.78

Table 11
City-level spatial and simulated cold-chain vulnerability indicators

Rank	City	Region	NRH	DNH (km)	DP	ARS	PRS	TRS	SDE	PHD (%)	CVS
19	Tripoli	Northwest	Tripoli	0.0	5	1.00	2	2	37.35	1.62	17.78
20	Misrata	Central coast	Misrata	0.0	4	1.00	2	2	35.55	0.64	17.04

Abbreviations**:** NRH = nearest reference hub; DNH = distance to nearest hub; DP = demand proxy; ARS = accessibility-risk score; PRS = power-risk score; TRS = transport-risk score; SDE = simulated disruption exposure; PHD = probability of high disruption; CVS = composite vulnerability score.

Note for Table 11. Distances are reported in kilometres. Demand proxy, power-risk score, and transport-risk score are ordinal screening scores from 1 to 5, where larger values indicate higher demand pressure or risk exposure. Simulated disruption exposure is the mean Monte Carlo score on a 0-100 scale. The probability of high disruption is the percentage of iterations that reach the threshold defined in Equation (7). The composite vulnerability score is calculated using Equation (9).

The city-level screening results show a distinct spatial gradient. Kufra records the highest composite vulnerability score because it combines the largest nearest-hub distance with high power-risk and transport-risk scores. Ghat, Ubari, Murzuq, and Sabha also appear among the highest-ranked locations because the model combines southern remoteness with higher infrastructure exposure and disruption intensity. This pattern provides a transparent basis for directing early resilience discussions toward southern and southeastern cities.

The lower scores recorded for coastal cities such as Tripoli, Benghazi, Misrata, Zawiya, Zliten, and Khoms reflect their proximity to reference hubs and their lower accessibility and operational-risk scores in the screening model. Their priorities are therefore likely to center on monitoring, maintenance, and data quality, while more remote cities require additional attention to redistribution time, maintenance access, and contingency planning. Figure 3 shows the screening-level composite cold-chain vulnerability across selected Libyan cities, while Figure 4 shows the top ten cities by simulated high-disruption probability.

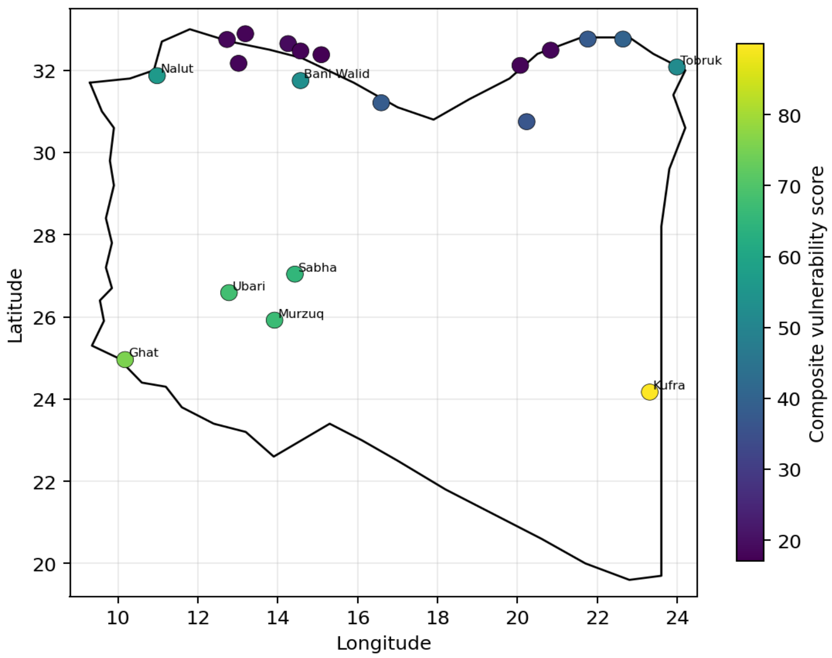

Fig. 3. Screening-level composite cold-chain vulnerability across selected Libyan cities

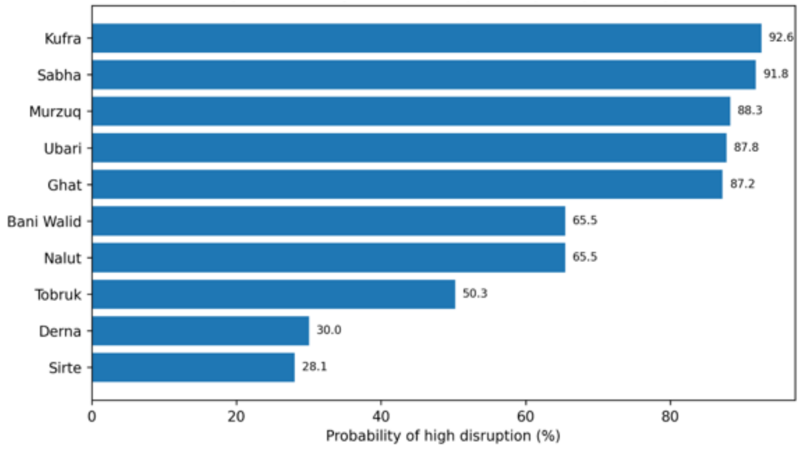

Fig. 4. Top ten cities by simulated high-disruption probability

The MCDM component shifts the analysis from the location of vulnerability to the prioritization of resilience strategies. The performance matrix is shown in Table 12. Scores are assigned on a 1-9 benefit scale according to the protocol reported in Section 2.5. The top-ranked strategy is the preventive maintenance and spare-parts programme (A4), with a TOPSIS closeness coefficient of 0.604. This result reflects its combined performance in risk reduction, cost efficiency, operational feasibility, and sustainability. It also addresses a practical concern in cold-chain systems: existing equipment may lose value when repairs, spare parts, and routine checks are not organized.

Digital temperature monitoring and alert systems (A3) rank second, with a closeness coefficient of 0.594. This strategy performs particularly well on the monitoring and data-improvement criterion and has relatively fast implementation potential. Route planning and emergency redistribution protocols (A5) rank third, with a coefficient of 0.590. This indicates that operational coordination can provide high value, particularly during campaigns, outbreaks, and temporary disruptions. Training and standard operating procedures (A6) rank fourth, reflecting strong affordability and speed but lower direct technical risk reduction compared with maintenance or monitoring.

Solar refrigerators (A1) and backup power solutions (A2) remain important, particularly for high-risk municipalities. Their lower system-wide ranks reflect cost, procurement, maintenance, and implementation requirements. The ranking therefore supports a combined approach: geographically targeted energy technologies alongside maintenance, monitoring, route planning, and training as system-wide strategies. Table 12 provides the strategy performance matrix, while Table 13 indicates the ranking of the strategies.

Table 12
Strategy performance matrix on a 1-9 benefit scale

Alternative	C1	C2	C3	C4	C5	C6	C7	C8
A1	9	8	4	4	6	3	8	7
A2	8	7	5	5	7	3	6	8
A3	7	6	7	8	7	9	7	8
A4	8	7	8	7	8	5	8	7
A5	7	8	8	8	7	6	6	9
A6	6	7	9	9	8	5	6	6
A7	6	8	7	8	8	4	6	9

Table 13
TOPSIS ranking of vaccine cold-chain resilience strategies

Rank	Alternative code	Strategy	TOPSIS closeness coefficient
1	A4	Preventive maintenance and spare-parts programme	0.604
2	A3	Digital temperature monitoring and SMS/online alert system	0.594
3	A5	Route planning and emergency redistribution protocol	0.590
4	A6	Training and standard operating procedures for vaccine handlers	0.537
5	A7	Passive cold boxes, conditioned ice packs, and emergency transport kits	0.457
6	A1	Solar direct-drive vaccine refrigerators for high-risk facilities	0.401
7	A2	Backup power units and voltage stabilization for municipal cold stores	0.344

Sensitivity analysis was conducted by changing the relative emphasis placed on risk-equity, feasibility-speed, cost efficiency, and emergency value. The top three strategies remain close across scenarios, although their internal order changes. Preventive maintenance and spare parts remain first in the tested scenarios, while digital monitoring and route planning remain within the top three. This stability check supports a priority strategy package that combines maintenance, monitoring, and operational redistribution protocols before or alongside targeted energy investments in the most vulnerable municipalities. Table 14 summarizes the sensitivity analysis.

Table 14
Sensitivity analysis of TOPSIS rankings under alternative weighting scenarios

Scenario	1st	2nd	3rd	Score 1st	Score 2nd	Score 3rd
Base	A4	A3	A5	0.604	0.594	0.590
Risk-equity dominant	A4	A5	A3	0.609	0.568	0.561
Feasibility-speed dominant	A4	A3	A5	0.611	0.606	0.603
Cost-efficiency dominant	A4	A5	A3	0.640	0.627	0.595
Emergency dominant	A4	A5	A3	0.599	0.596	0.595

3.1 Comparative validation and rank-reversal analysis

The TOPSIS ranking was compared with two additional ranking procedures: weighted-sum aggregation and WASPAS [21]. The same performance matrix and BWM-derived weights were used in all methods. Spearman and Kendall rank correlations were used to compare the TOPSIS ranking with the two benchmark rankings, as shown in Table 15.

Table 15
Comparative validation of strategy rankings

Alternative	TOPSIS rank	Weighted-sum rank	WASPAS rank
A1	6	6	6
A2	7	7	7
A3	2	3	3
A4	1	1	1
A5	3	2	2
A6	4	4	4
A7	5	5	5
Spearman correlation with TOPSIS	-	0.964	0.964
Kendall correlation with TOPSIS	-	0.905	0.905

The validation results show strong agreement between TOPSIS and the two benchmark procedures. A4 remains the first-ranked strategy in all three methods, while A3 and A5 remain within the top three. The small difference between A3 and A5 indicates that these two strategies are closely competing priorities rather than sharply separated options.

The rank-reversal analysis identifies the conditions under which the first-ranked strategy changes. A4 is stable when risk reduction, cost efficiency, operational feasibility, and sustainability receive base or higher emphasis. A3 becomes first when the monitoring and data-improvement criterion receives higher emphasis, while A5 becomes first when spatial equity or emergency response value receives substantially higher emphasis. The practical conclusion is therefore a leading package formed by A4, A3, and A5, with final ordering depending on the emphasis given to monitoring, equity, and emergency response, as shown in Table 16.

Table 16
Rank-reversal thresholds under one-at-a-time weight variation

Criterion varied	Multiplier range tested	Observed first-ranked strategy
C1 Risk reduction	0.20-0.58	A5
C1 Risk reduction	0.59-0.91	A3
C1 Risk reduction	0.92-3.00	A4
C2 Spatial equity	0.20-0.75	A3
C2 Spatial equity	0.76-1.32	A4
C2 Spatial equity	1.33-3.00	A5
C3 Cost efficiency	0.20-0.84	A3
C3 Cost efficiency	0.85-3.00	A4
C6 Monitoring/data improvement	0.20-1.04	A4
C6 Monitoring/data improvement	1.05-3.00	A3
C8 Emergency response value	0.20-1.91	A4
C8 Emergency response value	1.92-3.00	A5

Note: For each test, the selected criterion weight was multiplied by the stated value and all weights were renormalized to sum to one.

A key managerial implication is that cold-chain resilience requires more than equipment procurement. Refrigerators, generators, and solar devices remain important, but the model highlights the system-wide value of maintenance, spare parts, monitoring, and redistribution protocols. This is particularly relevant in settings where equipment may exist but lose functionality because repairs, voltage protection, spare parts, or temperature visibility are not consistently organized. The first priority is therefore to keep existing assets functional and observable before expanding asset stock.

A second implication concerns spatial equity. Strategies should be evaluated not only by aggregate national benefit but also by their effect on remote municipalities. The vulnerability map indicates that cities in the south and southeast may require targeted support even if their population size is smaller than coastal cities. This is important because vaccine-preventable disease risk is shaped by both population concentration and service accessibility. A strategy that protects remote populations may be socially valuable even if it is not the cheapest intervention per dose at the national level.

A third implication is that digital monitoring should be treated as both a technical strategy and a data-improvement strategy. Temperature loggers, alerts, and reporting dashboards can reduce response time when refrigerators fail or transport is delayed, while also generating records that improve future planning. In this sense, digital monitoring can help move the system from structured screening toward evidence-based management.

4. Conclusions

This paper proposed a spatial-simulation-MCDM framework for organizing spatial, disruption, and expert-elicited evidence on vaccine cold-chain resilience in Libya. The framework combines calculated city-level accessibility measures, structured operational-risk screening, Monte Carlo disruption simulation, BWM-based criterion weighting, and TOPSIS ranking into a transparent workflow. It offers a practical way to connect where cold-chain vulnerability is concentrated with which resilience strategies should receive early attention.

The case application places Kufra, Ghat, Ubari, Murzuq, and Sabha among the locations requiring early resilience attention. At the strategy level, preventive maintenance and spare parts, digital temperature monitoring, and route planning with emergency redistribution protocols form the leading package. These actions complement targeted energy investments and provide practical starting points for improving reliability, continuity, and equity while facility-level data are expanded.

Author Contributions

Conceptualization, I.B; writing—original draft preparation, I.B. and O.S; writing—review and editing, I.B.; visualization, I.B. and O.S; supervision, I.B.; project administration, I.B. All authors have read and agreed to the published version of the manuscript.

Funding

This research received no external funding.

Data Availability Statement

The study did not report any data.

Conflicts of Interest

The authors declare that they have no known competing financial interests or personal relationships that could have appeared to influence the work reported in this paper.

Acknowledgement

This research was not funded by any grant.

References

[1] Jamwal, A., Vijayvargy, L., Gupta, S., Sahoo, S. K., & Sarma, P. R. S. (2026). A decision-making framework for improving vaccine supply chain performance and sustainability. International Journal of Productivity and Performance Management, 75(5), 1496–1520. https://doi.org/10.1108/IJPPM-05-2025-0395

[2] Hay, M., Teichert, A., Kilz, S., & Vosen, A. (2025). Resilience in the vaccine supply chain: Learning from the COVID-19 pandemic. Vaccines, 13(2), 142. https://doi.org/10.3390/vaccines13020142

[3] Alossta, A., Elmansouri, O., & Badi, I. (2021). Resolving a location selection problem by means of an integrated AHP-RAFSI approach. Reports in Mechanical Engineering, 2(1), 135–142. https://doi.org/10.31181/rme200102135a

[4] World Health Organization Regional Office for the Eastern Mediterranean. (2025). With WHO support, Libya launches a comprehensive review of its National Immunization Programme. https://www.emro.who.int/lby/libya-news/with-who-support-libya-launches-a-comprehensive-review-of-its-national-immunization-programme.html

[5] Abusrewil, S., Almgadmi, A., Eljerbi, A., Hadid, I., Sherif, M., Ben Suoud, A., Ben Ramadan, M., Kabouka, M., Ben Omer, E., Elkout, H., Ehnaish, S., Ibrahim, M., Belkhair, B., & Alhudiri, I. (2025). Evolution of the Libyan Expanded Programme of Immunization. Libyan Medical Journal, 17(1), 1–4. https://doi.org/10.69667/lmj.2517101

[6] Allen, L. N., Hatefi, A., Kak, M., Herbst, C. H., Mallender, J., & Karem, G. (2024). A rapid mixed-methods assessment of Libya's primary care system. *BMC Health Services Research*, *24*(1), 721.. https://doi.org/10.1186/s12913-024-11121-w

[7] Pambudi, N. A., Sarifudin, A., Gandidi, I. M., & Romadhon, R. (2022). Vaccine cold chain management and cold storage technology to address the challenges of vaccination programs. Energy Reports, 8, 955–972. https://doi.org/10.1016/j.egyr.2021.12.039

[8] Yang, Y., Bidkhori, H., & Rajgopal, J. (2021). Optimizing vaccine distribution networks in low and middle-income countries. Omega, 99, 102197. https://doi.org/10.1016/j.omega.2020.102197

[9] UNICEF Supply Division. (2019). Cold chain equipment: Solar direct drive and mains powered refrigerators. https://www.unicef.org/supply/sites/unicef.org.supply/files/2019-06/cold-chain-equipment-sdd-drive-and-mains-powered-refrigerators.pdf

[10] Feyisa, D. (2021). Cold chain maintenance and vaccine stock management practices at public health centers providing child immunization services in Jimma Zone, Oromia Regional State, Ethiopia: Multi-centered, mixed method approach. Pediatric Health, Medicine and Therapeutics, Volume 12, 359–372. https://doi.org/10.2147/PHMT.S312039

[11] Cao, Y., Li, T., Chen, H., Zhao, Q., Sun, J., Grepin, K. A., & Kang, J. Y. (2025). Evaluating geographic accessibility to COVID-19 vaccination across 54 countries/regions. BMJ Global Health, 10(2), e017761. https://doi.org/10.1136/bmjgh-2024-017761

[12] Azadi, Z., Eksioglu, S. D., & Geismar, H. N. (2024). Optimization of pediatric vaccines distribution network configuration under uncertainty. Computers & Industrial Engineering, 192, 110230. https://doi.org/10.1016/j.cie.2024.110230

[13] Tirkolaee, E. B., Torkayesh, A. E., Tavana, M., Goli, A., Simic, V., & Ding, W. (2023). An integrated decision support framework for resilient vaccine supply chain network design. Engineering Applications of Artificial Intelligence, 126, 106945. https://doi.org/10.1016/j.engappai.2023.106945

[14] Bouraima, M. B., *et al.* (2024a). An integrated multi-criteria approach to formulate and assess healthcare referral system strategies in developing countries. Healthcare Analytics, 5, 100315. https://doi.org/10.1016/j.health.2024.100315

[15] Bouraima, M. B., *et al.* (2024b). Sustainable healthcare system devolution strategy selection using the AROMAN MCDM approach. Spectrum of Decision Making and Applications, 1(1), 46–63. https://doi.org/10.31181/sdmap1120243

[16] Badi, I., & Ballem, M. (2018). Supplier selection using the rough BWM-MAIRCA model: A case study in pharmaceutical supplying in Libya. Decision Making: Applications in Management and Engineering, 1(2), 16–33. https://doi.org/10.31181/dmame1802016b

[17] Hien, D. N., & Thanh, N. V. (2022). Optimization of cold chain logistics with fuzzy MCDM model. Processes, 10(5), 947. https://doi.org/10.3390/pr10050947

[18] Rezaei, J. (2015). Best-worst multi-criteria decision-making method. Omega, 53, 49–57. https://doi.org/10.1016/j.omega.2014.11.009

[19] Rezaei, J. (2016). Best-worst multi-criteria decision-making method: Some properties and a linear model. Omega, 64, 126–130. https://doi.org/10.1016/j.omega.2015.12.001

[20] Ekici, U., Akay, M. E., & Moslem, S. (2026). Determination of logistics center locations in Türkiye using AHP-based TOPSIS methods. Transportation Research Interdisciplinary Perspectives, 37, 101967. https://doi.org/10.1016/j.trip.2026.101967

[21] Zavadskas, E. K., Turskis, Z., Antucheviciene, J., & Zakarevicius, A. (2012). Optimization of weighted aggregated sum product assessment. Elektronika ir Elektrotechnika, 122(6), 3–6. https://doi.org/10.5755/j01.eee.122.6.1810